

# Improved Knowledge of SAR Geometry through Atmospheric Modelling

Michael Jehle, Othmar Frey, David Small, Erich Meier, Daniel Nüesch  
Remote Sensing Laboratories, University of Zurich, Winterthurerstrasse 190; CH-8057 Zurich, Switzerland  
Email: michael.jehle@geo.unizh.ch

## Abstract

Satellites observing and measuring the Earth's surface with electromagnetic waves are subject to atmospheric path delays. These atmospheric effects on radar signal propagation modify the signal velocity and direction and can be considered by simple modeling. In order to increase the geolocation accuracy of spaceborne SAR applications we developed a software tool that accounts for atmospheric path delays. Well-calibrated spaceborne ENVISAT-ASAR data are used to investigate improvements to knowledge of the geometry of the scene.

## 1 Introduction

Knowledge of range and azimuth in spaceborne SAR has improved in recent years. Regarding geometric accuracy, the importance of atmospheric path delay increases as well with continuing improvements to the resolution of SAR systems surveying the Earth and other planets. Contributions of path delay of the atmosphere must be respected in order to be able to get an atmosphere-independent geolocation accuracy in the range of approximately one meter. This motivated a study dedicated to geometric error budget analysis for the upcoming of the TerraSAR-X satellite [1].

Atmospheric path delay contributions are mainly due to ionospheric and tropospheric influences. At X-band frequencies, ionospheric path delay can amount [1] to up to 1 m and tropospheric delay up to 3 m only for propagation from the satellite to the Earth. For SAR systems this delay can add up to 16 m, when one compares two way path delays between ascending / descending acquisition geometries.

The most important contributions caused by the ionosphere and the troposphere are described in sections 2 and 3. Section 4 discusses path delays of a well-calibrated ENVISAT-ASAR scene calculated with the newly developed software tool. In the last section conclusions and recommendations are made.

## 2 Ionospheric Delay

The ionosphere located at a height of approximately 50 km - 1500 km is characterized by the existence of free electrons and ions that define the refractive index in this area. The degree of ionisation is caused mainly by solar UV radiation and depends on the local atmospheric density. The

Total Electron Content (TEC) specifies the number of free electrons in a column of  $1 \text{ m}^2$  along the signal path. TEC Units (TECU) are  $10^{16}$  electrons per  $\text{m}^2$ . TEC is usually low at night and highest at about 14:00 local time, when solar radiation is approximately two hours past zenith. This two hour shift depends on the time light needs to ionise the layer to the maximum.

The degree of ionisation or the number of free electrons interacting with the traversing signal causes a path delay that depends on the signal's frequency  $f$ . This dispersive behaviour can be used to estimate the TEC along the path. GPS stations, for example, measure the time delay at L1 and L2 frequencies, calculate over a network of receiving stations global TEC and provide GPS users with ionosphere correction terms through the navigation message. Daily maps of global TEC are published on the internet (e.g. [www.aiub.unibe.ch/ionosphere/](http://www.aiub.unibe.ch/ionosphere/)). Based on [2], one can describe the path delay  $\Delta\Psi_{iono,SAR}$  through the ionosphere for electromagnetic waves traveling from a satellite to the Earth and back by:

$$\Delta\Psi_{iono,SAR} = 2 \cdot K \cdot \frac{TEC}{f^2 \cdot \cos \alpha_{offNd}}. \quad (1)$$

The factor  $\frac{1}{\cos \alpha_{offNd}}$  accounts for the slant range direction.  $\alpha_{offNd}$  [degrees] denotes the satellite off-nadir angle, and  $K = 40.28 \left[ \frac{\text{m}^3}{\text{s}^2} \right]$  is a refractive constant [2]. Path delays for X-band frequencies can be in the range of up to 2 m for propagation through the ionosphere to the Earth and back. Estimating a total path delay for spaceborne SAR applications, one has to consider additionally that ascending (ASC) / descending (DSC) intercomparisons double the effect of the error! Predicting or extrapolating TEC is difficult due to the high variability of the ionosphere. An approach for a global TEC prediction model, looking for a few days into the future was developed by [3]. The

basic idea is to extend the Klobuchar model [4] that estimates TEC using a daily cosine function, with periodic parameters that influence the daily TEC. According to measurements, it is mainly the periodicity due to the 11 year solar cycle, the lunar cycle and annual- and semi-annual variations. Extrapolating and estimating a trend function of this parameters leads to a stand-alone TEC prediction model that is implemented as an optional feature in the software tool for SAR applications. The accuracy of this stand-alone model for predictions over long time periods is low due to the ionosphere's variability.

**Figure 1** shows on the left (Figure 1a) an example of atmospheric path delay for a C-band ENVISAT-ASAR IS7 scene acquired on January 22th 2003 at 9:29. Modeled TEC was 18 TECU in zenithal direction and off-nadir angle was from 36.7 to 39.3 degrees. Calculated path delays range from 0.63 m to 0.66 m increasing with the growing off-nadir angle. On the right in Figure 1b the calculated total atmospheric path delay is outlined. It can clearly be seen, that the total path delay depends strongly on topography. The total path delay for C-band is typically in the range of 5 m to 7 m.

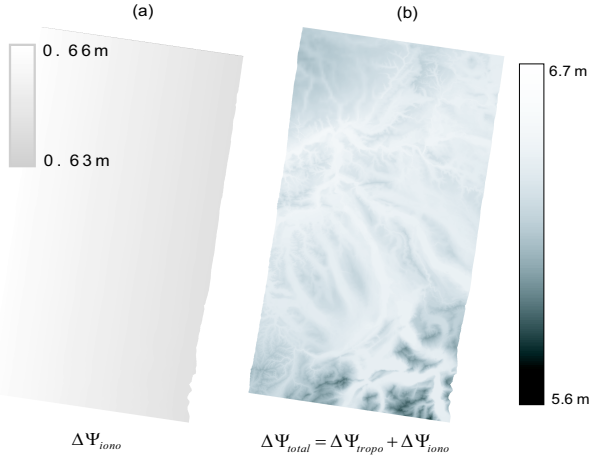


**Figure 1:** Ionospheric- (left) vs. total path delay (right).

### 3 Tropospheric Delay

Tropospheric path delay is caused by variations in the refractive index  $n$  as a function of the parameters air pressure  $P$ , temperature  $T$  and water vapour pressure  $e$ . Based on basic principles of Saastamoinen [5] and Hopfield [6], the idea of modeling tropospheric path delay  $\Delta\Psi_{tropo,SAR}$  is to separate the delay into a hydrostatic  $\Delta\Psi_{hyd,SAR}$ , a wet  $\Delta\Psi_{wet,SAR}$ , and a liquid  $\Delta\Psi_{liq,SAR}$  component as follows:

$$\Delta\Psi_{tropo,SAR} = \Delta\Psi_{hyd,SAR} + \Delta\Psi_{wet,SAR} + \Delta\Psi_{liq,SAR} \quad (2)$$

The hydrostatic component refers to a standard atmosphere. The wet and liquid components model the difference between the standard and actual atmosphere. The

wet component accounts for the water vapour while the liquid component considers the liquid water content (clouds, droplets) along the signal path. Due to its small contribution (at cm level)  $\Delta\Psi_{liq,SAR}$  can generally be neglected for SAR applications.  $\Delta\Psi_{hyd,SAR}$  can be modeled in the zenithal direction according to [2]:

$$\Delta\Psi_{hyd,SAR} = 2 \cdot 10^{-6} k_1 \cdot \frac{R_d}{g_m} P_s. \quad (3)$$

with  $g_m$  the local gravity, the refractive constant  $k_1=77.6 [\frac{K}{mbar}]$  and gas constant  $R_d=287 [\frac{J}{K \cdot kg}]$ . For the measured surface air pressure  $P_s$ , the hydrostatic delay can be predicted with an accuracy of 1 mm [7].

Wet path delay can not be modeled as well as hydrostatic delay. A widely used approach for zenithal wet path delay  $\Delta\Psi_{wet}$  was published by [8]. For SAR applications it must be multiplied by a factor of 2 to amount for two-way propagation:

$$\Delta\Psi_{wet,SAR} = 2 \cdot 10^{-6} \cdot \left( \frac{(k'_2 T_m + k_3) R_d e_0}{T_0 (g_m (\lambda + 1) - \beta R_d)} \right) \cdot \kappa_{wet} \quad (4)$$

with:

$$\kappa_{wet} = \left( 1 - \frac{\beta h}{T_0} \right)^{\frac{(\lambda+1)g_m}{R_d \beta} - 1} \quad (5)$$

where  $k'_2 = 23.3 [\frac{K}{mbar}]$ ,  $k_3 = 3.75 \cdot 10^5 [\frac{K^2}{mbar}]$  are refractive constants,  $\beta = 6.5 [\frac{K}{km}]$  is the temperature lapse rate,  $T_0$  [K],  $e_0$  the temperature-, water vapour pressure above sea level,  $T_m$  [K] the mean temperature of water vapour,  $h$  the target's height and  $\lambda$  [unitless] the average decrease of water vapour. Parameters  $T$ ,  $P$ ,  $e$ ,  $\lambda$ ,  $\beta$  are modeled [7] considering target height  $h$ , latitude and day of the year. For every parameter a look up table is calculated accounting for variations of mean  $T$ ,  $P$ ,  $e$ ,  $\lambda$ ,  $\beta$  above sea level regarding different latitudes. The slant range propagation is calculated by dividing  $\Delta\Psi_{tropo,SAR}$  by  $\cos \alpha_{OffNad}$ .

**Figure 2** shows an example of tropospheric path delay for the ENVISAT-ASAR scene over Lucerne / Zurich.

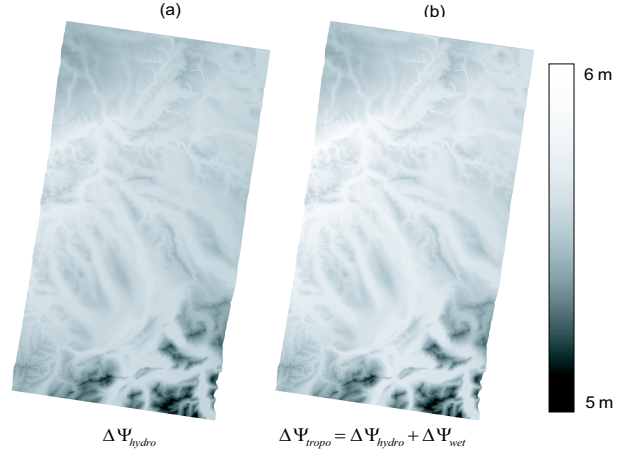


**Figure 2:** Hydrostatic- (left) vs. tropospheric path delay (right).

Tropospheric path delay for SAR applications is usually in the range of 4.6 to 5.4 m for hydrostatic path delay and 0 to 0.8 m for wet path delay. It can be clearly seen that in the higher regions at the lower right path delay is about 1 m smaller than in flatter areas in the north. It is evident that, under constant atmospheric conditions, path delay depends mainly on the target's surface height.

## 4 Discussion

Using the presented contributions and models for calculating path delay of electromagnetic waves propagating through the atmosphere, we developed a software tool to calculate pixel based path delays for spaceborne L to X-band SAR / radar applications. Even short range atmospheric path delay predictions with an estimated accuracy of at least 50% are possible using an optional ionosphere model in the software.

Figure 1 and 2 show calculated path delay examples from the developed software of an ENVISAT-ASAR scene.

Figure 1 juxtaposes the contribution of the ionospheric path delay and the total path delay. The typical drift in Figure 1a of path delay increasing from the right to the left results from the growing off-nadir angle between satellite and calculated target pixel. The calculated total atmospheric path delays of the scene in Figure 1b are typical for C-band frequencies.

Figure 2a and 2b show the path delays due to the troposphere. While the hydrostatic delay in Figure 2a clearly shows the terrain of the scene, the wet delay has mainly the same behaviour as ionospheric delay (drift to higher amounts with growing off-nadir angle) and is therefore a nearly constant contribution. Figure 2b presents the tropospheric delay  $\Delta\Psi_{tropo,SAR} = \Delta\Psi_{hydr,SAR} + \Delta\Psi_{wet,SAR}$ . The difference between Figure 2a and 2b is mainly a shift in scale, visible as a small difference in brightness.

The software is intended to calculate atmospheric path delays for TerraSAR-X. Total path delays for X-band frequencies would be approximately 0.4 m smaller due to the smaller influence of the ionosphere at that shorter wavelength. The presented ENVISAT-ASAR example demonstrates the adaptive and comparative capabilities of the tool.

## 5 Conclusions

High resolution SAR sensors such as the upcoming TerraSAR-X depend on accurate data calibration in order to provide the most accurate geolocation possible. Atmo-

spheric path delays therefore have to be considered [1]. We developed a software tool with the presented models and path delay contributions that calculates for spaceborne SAR / radar applications the expected path delay for every single pixel within a scene. This software tool is designed to be easily integrated into other software environments enabling improved a-priori knowledge of the geometry of a SAR acquisition.

## 6 Acknowledgement

This work was funded by the German Aerospace Center (DLR) through Contract No. 523/65655831.

## References

- [1] Frey, O.; Small D.; Meier E.; Nüesch D. and Achim Roth: *Geometric Error Budget Analysis for TerraSAR-X*. Proc. EUSAR, 2004.
- [2] Hanssen, R. F.: *Radar Interferometry*. Vol.2, Dordrecht, Boston, London: Kluwer Academic Publishers, 2001.
- [3] Schaer, S.: *Mapping and Predicting the Earth's Ionosphere using the Global Positioning System*. Geodätisch- geophysikalische Arbeiten in der Schweiz, 1999.
- [4] Klobuchar, J.A.: *Ionospheric Time Delay Algorithm for Single Frequency GPS Users*. IEEE Transactions on Aerospace and Electronic Systems, Vol. 23, pp. 325-331, 1987.
- [5] Saastamoinen, J.: *Contributions to the Theory of Atmospheric Refraction*. Bulletin Geodesique, No. 105, No. 106, No. 107, 1973.
- [6] Hopfield, H.: *Tropospheric Range Error at Zenith*. Committee on Space Research, 14th Plenary Meeting, working group 1, id. number a.15, edited by Applied Physics Laboratory, The Johns Hopkins University, Maryland, 1971.
- [7] Collins, P. and Langley, R.: *Limiting Factors in Tropospheric Propagation Delay Error Modelling for GPS Airborne Navigation*. The Institute of Navigation 52nd Annual Meeting, Cambridge, USA, 1996.
- [8] Askne, J. and Nordius, H.: *Estimation of Tropospheric Delay for Microwaves from Surface Weather Data*. Radio Science, Vol. 22, No. 3, pp. 379- 386, 1987.